Vol 13 No 4, April 2004
1009-1963/2004/13(04)/0473-08

Chinese Physics

© 2004 Chin. Phys. Soc.
and IOP Publishing Ltd

Luminescence of $Ba_{0.85}MgAl_{10}O_{16.94}:Eu^{2+}_{0.09}$ with different fluxes*

Deng Chao-Yong(邓朝勇)[a)b)†], He Da-Wei(何大伟)[a)], Zhuang Wei-Dong(庄卫东)[b)], Wang Yong-Sheng(王永生)[a)], Kang Kai(康 凯)[a)b)], and Huang Xiao-Wei(黄小卫)[b)]

[a)] *Laboratory of Materials for Information Storage and Display, Institute of Optoelectronic Technology, Beijing Jiaotong University, Beijing* 100044, *China*

[b)] *National Engineering Research Center for Rare Earth Materials, General Research Institute for Nonferrous Metals, Beijing* 100088, *China*

(Received 18 August 2003; revised manuscript received 13 October 2003)

$BaMgAl_{10}O_{17}:Eu^{2+}$, known as BAM, is a very important blue-emitting phosphor used in plasma display panels (PDP) and three band fluorescent lamps. In this paper, the $Ba_{0.85}MgAl_{10}O_{16.94}:Eu^{2+}_{0.09}$ phosphors with different fluxes (BaF_2, MgF_2, AlF_3, $BaCl_2$, $MgCl_2$, $AlCl_3$, H_3BO_3) were prepared by high temperature solid-state reaction method and the influence of different fluxes on the luminescence of $Ba_{0.85}MgAl_{10}O_{16.94}:Eu^{2+}_{0.09}$ phosphor was studied under 254nm excitation and vacuum ultraviolet (VUV) excitation. It was found that fluorides have better flux effects than chlorides and H_3BO_3. The mechanism of particle growth in the presence of flux in the process of phosphor preparation is discussed in detail. Particle size distribution and the crystal structure of the phosphors are also analysed.

Keywords: flux, mechanism of particle growth, luminescence, VUV excitation
PACC: 3250, 7855, 7820

1. Introduction

Barium magnesium aluminate ($BaMgAl_{10}O_{17}$) activated by divalent europium ions (Eu^{2+}), known as $BaMgAl_{10}O_{17}:Eu^{2+}$(BAM), is widely used as a blue-light-emitting commercial phosphor for three band fluorescent lamps and plasma display panels (PDP) due to its high efficiency and good chromaticity.[1−4] This phosphor has a broad band emission with the peak at near 450nm owing to the $4f^65d$–$4f^7$ transition of the Eu^{2+} ion both under 254nm excitation and vacuum ultraviolet excitation.[5,6]

This phosphor has a crystal structure similar to hexagonal β-alumina, which is well known in $Na_2O{\cdot}11Al_2O_3$ compound. The matrix crystal is composed of the replacement of Na^+ by Ba^{2+} and of the partial replacement of Al^{3+} by Mg^{2+} in the $Na_2O{\cdot}11Al_2O_3$ crystal, thus attaining the electric charge compensation. The Eu^{2+} activator is generally thought to situate at Ba^{2+} site. But Mishra *et al* recently reported that Eu^{2+} activator probably occupies multiple sites: the Beevers–Ross (BR) site, mid-oxygen (mO) site and anti-Beevers–Ross (a-BR) site.[1,7,8]

Many efforts have been made to elucidate the crystal structure and phase relation, and many researchers have successfully prepared various analogues of these compounds including single crystals.[3,9] These research efforts have been facilitated by the practical application of these phosphors such as fluorescent lamps, display devices and so on. Smets *et al* have found a true single phase to take the form $BaMgAl_{10}O_{17}$, which showed good consistent performances, both in the lamp manufacturing process and in lamp operation.[10,11] However, with respect to the composition of this efficient blue-emitting phosphor used in lamps and plasma displays, the literature is somewhat ambiguous. Phosphors with similar but not identical composition were prepared by high temperature solid-state reaction method including $Ba_2Mg_2Al_{22}O_{37}$ (emission at 449nm),[12] $BaMg_2Al_{16}O_{27}$(emission at 450nm)[6] and recently

*Project supported by the National Natural Science Foundation of China (Grant Nos 50204002 and 50272013) and the Natural. Science Foundation of Beijing (Grant No 4012010).

†E-mail address: chydeng@center.njtu.edu.cn, chydeng@vip.sina.com

$BaMg_3Al_{14}O_{25}$ prepared by hydrothermal reaction, which emits at 467nm.[13] Some researchers have investigated the luminescence properties of BAM phosphors with different Mg^{2+}, Al^{3+} content and phosphors with non-stoichiometric ratio were reported in the literature.[14] The luminescence properties of these phosphors with different Ba^{2+} content were also studied in our previous work. It was found that Ba^{2+} content has an evident influence on the luminescence performance of these phosphors, and when x=0.94 there is a maximum in the relative emission intensities in $Ba_{x-y}MgAl_{10}O_{16+x}:Eu_y^{2+}$ phosphors.

In the process of phosphor preparation, some substances are added deliberately to help crystal growth. These substances, which are reactants added deliberately to the raw materials, are called fluxes. Fluxes are usually compounds of alkali-or alkaline earth metals having low melting points. The halides are most frequently used.[15] The flux plays a determining role in the process of particle growth and each flux influences the particle size and shape in a different way. Therefore, a combination of fluxes is sometimes used to obtain products with desired morphology. The selection of flux generally sticks to two principles: one is that the melting point of flux is lower than the reaction temperature; and the other is that impurity ions would not be introduced.

In our experiment, the $Ba_{0.85}MgAl_{10}O_{16.94}:Eu_{0.09}^{2+}$ phosphors with different fluxes (BaF_2, MgF_2, AlF_3, $BaCl_2$, $MgCl_2$, $AlCl_3$, H_3BO_3) were prepared by high temperature solid-state reaction and the influence of different fluxes on the luminescence of $Ba_{0.85}MgAl_{10}O_{16.94}:Eu_{0.09}^{2+}$ phosphor was studied under 254nm excitation and vacuum ultraviolet (VUV) excitation. It was found that the fluorides and chlorides have a different flux effect on $Ba_{0.85}MgAl_{10}O_{16.94}:Eu_{0.09}^{2+}$ phosphors. H_3BO_3 was also studied as flux for comparison. A possible mechanism on the function of flux was proposed and discussed in detail. Particle size distribution and the crystal structure of the phosphors were also analysed.

2. Experimental procedure

The samples were prepared using $BaCO_3$ (G.R.), MgO (G.R.), $Al(OH)_3$ (G.R.), Eu_2O_3 (G.R.) as starting materials. The fluxes were introduced from BaF_2 (G.R.), MgF_2 (G.R.), $AlF_3{\cdot}3.5H_2O$ (G.R.), $BaCl_2{\cdot}2H_2O$ (G.R.), $MgCl_2{\cdot}6H_2O$ (G.R.), $AlCl_3{\cdot}6H_2O$ (G.R.) and H_3BO_3 (G.R.). Appropriate quantities of the raw materials were mixed according to the formula $Ba_{0.85}MgAl_{10}O_{16.94}:Eu_{0.09}^{2+}$ and the concentration of fluxes was determined according to the ratios of 10 at.% metal cations from flux compounds to the same type cations in host materials and the concentration of H_3BO_3 used as flux is 0.1 mole per mole of host. Only one type of flux was used in each sample. And then the mixture of raw materials (including the fluxes) was ground in an agate mortar carefully and fired at 1550°C in CO reducing atmosphere for 4h.

X-ray powder diffraction data were collected using a MXP21VAHF-M21X X-ray diffractometer having a Cu$K\alpha$ radiation with the application of an electric current of 250mA at an accelerating voltage of 40kV. A SPEX fluoroMAX-2 spectrofluorometer was used to measure the excitation and emission spectra of photoluminescence and the chromaticity monitored by an SPR-920C spectroradiometer. The luminous characteristics under VUV excitation were measured with the help of a PDP-II VUV spectroradiometer. A Coulter Multisizer II granularity analyser was used to analyse the particle size distribution.

3. Results and discussion

3.1. Crystal structure

The Ba-poor hexa-aluminate and $BaMgAl_{10}O_{17}$ can form solid solutions because both have exactly the same structure of β-alumina.[11] X-ray diffraction spectra of the samples in our experiment at 1550°C firing temperature are shown in Fig.1. Compared with the JCPDS card 26–0163, only a single phase with the β-alumina structure is observed and no extraneous phase is found. All these spectra are quite similar to each other regardless of the flux type. It is argued that this single phase has been developed fully in our preparation conditions and all the samples have the single β-alumina structure and similar crystallinities regardless of the flux type.

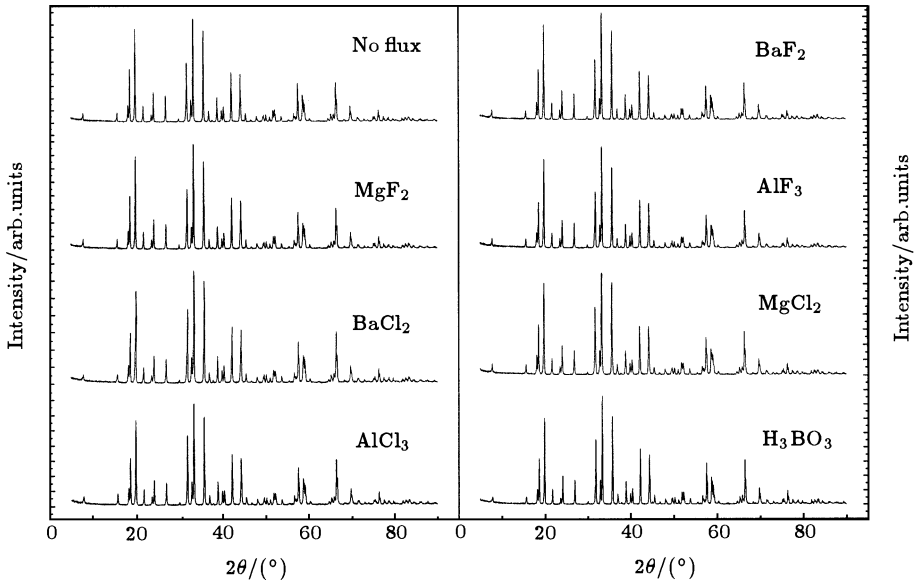


Fig.1. XRD spectra of $Ba_{0.85}MgAl_{10}O_{16.94}:Eu^{2+}_{0.09}$ with different fluxes (T=1550°C).

JCPDS card 26–0163 furnishes the cell parameters of the hexagonal $BaMgAl_{10}O_{17}$ phase: a=0.562nm, c=2.264nm, c/a=4.0280, v=0.6193nm^3. The x-ray diffraction data in our experiment were indexed using the program TREOR90. Table 1 shows the indexing results of $Ba_{0.85}MgAl_{10}O_{16.94}:Eu^{2+}_{0.09}$ with different fluxes at different firing temperatures. All diffraction peaks have been indexed in all samples. A careful examination of data in Table 1 shows that there is a similar tendency in a and c with the change of flux type. The parameter c is roughly proportional to a: that is, when there is a larger a, there is also a corresponding larger c; this must result in a larger cell volume (v), which can be seen from Fig.2. In addition, further investigation reveals that the c/a ratio is connected with the firing temperature. No matter what type flux is selected, the c/a ratio is smaller at higher firing temperature than that at lower firing temperature, as showed in Fig.3. When the samples are fired at 1550°C, the c/a ratios are smaller than the ones fired at 1400°C regardless of the flux type. It is notable that when no flux is used the sample has a largest c/a ratio and with H_3BO_3 as flux there is a smallest c/a ratio at the same firing temperature. Other parameters change in a similar manner for the samples without any flux and with H_3BO_3 as flux. All the c/a ratios changed in a small range (4.0189–4.0242) and there is no abrupt change in the c/a ratio (space group $P6_3/mmc$), which confirms that all these samples have the same crystal structure as β-alumina.[11,12]

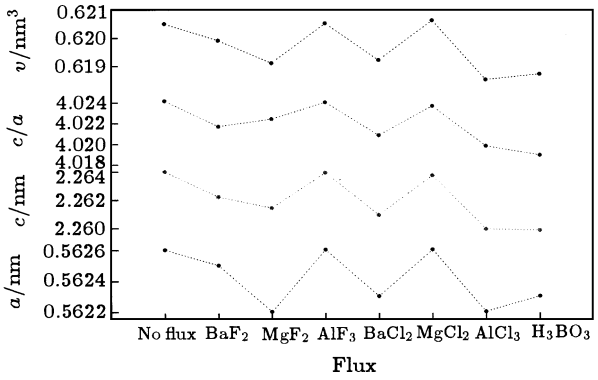


Fig.2. Cell parameters of $Ba_{0.85}MgAl_{10}O_{16.94}:Eu^{2+}_{0.09}$ with different fluxes (T=1550°C).

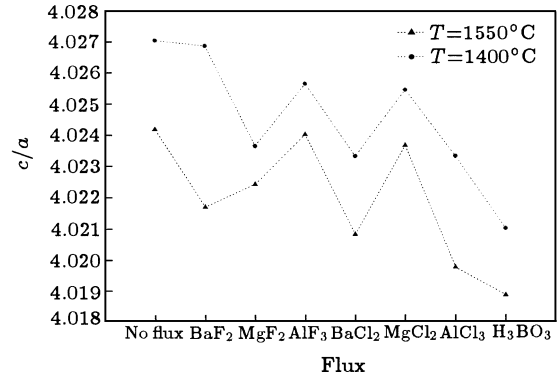


Fig.3. The c/a ratios of $Ba_{0.85}MgAl_{10}O_{16.94}:Eu^{2+}_{0.09}$ with different fluxes.

Table 1. XRD data index results of $Ba_{0.85}MgAl_{10}O_{16.94}:Eu^{2+}_{0.09}$ with different fluxes.

Flux	Cell Parameters (fired at 1550°C)				Cell Parameters (fired at 1400°C)			
	a/nm	c/nm	c/a	v/nm^3	a/nm	c/nm	c/a	v/nm^3
No Flux	0.5626	2.2640	4.0242	0.6205	0.5623	2.2644	4.0270	0.6201
BaF_2	0.5625	2.2622	4.0217	0.6199	0.5624	2.2647	4.0269	0.6204
MgF_2	0.5622	2.2614	4.0224	0.6191	0.5629	2.2649	4.0236	0.6214
AlF_3	0.5626	2.2639	4.0240	0.6205	0.5620	2.2624	4.0256	0.6188
$BaCl_2$	0.5623	2.2609	4.0208	0.6192	0.5624	2.2627	4.0233	0.6197
$MgCl_2$	0.5626	2.2637	4.0236	0.6206	0.5625	2.2643	4.0254	0.6204
$AlCl_3$	0.5622	2.2599	4.0197	0.6185	0.5623	2.2623	4.0233	0.6191
H_3BO_3	0.5623	2.2598	4.0189	0.6187	0.5621	2.2602	4.0210	0.6185

3.2. Particle size distribution

Practical phosphors must be prepared so that they can form a dense, pinhole-free coating on a substrate. This property is determined mainly by particle size distribution and surface treatment.[16] For fluorescent lamp phosphors, the optimum coating thickness is roughly proportional to its mean particle size: the smaller the particle size, the thinner the coating can be. However, when a phosphor is prepared in a condition that yields fine particles, luminescence efficiency of the product tends to become lower. Phosphors having a small particle size and high efficiency would be most useful.

Table 2. Particle size distribution of $Ba_{0.85}MgAl_{10}O_{16.94}:Eu^{2+}_{0.09}$ with different fluxes.

Flux	Fired at 1550°C			Fired at 1400°C		
	Mean/μm	Median/μm	Mode/μm	Mean/μm	Median/μm	Mode/μm
No Flux	5.250	5.278	6.023	5.224	5.271	5.030
BaF_2	5.789	5.909	6.367	5.662	5.723	6.637
MgF_2	6.306	6.452	6.637	5.614	5.737	5.698
AlF_3	6.264	6.440	7.213	6.400	6.496	6.279
$BaCl_2$	4.428	4.646	5.244	4.928	4.997	5.778
$MgCl_2$	4.496	4.751	5.940	4.591	4.793	5.466
$AlCl_3$	4.939	4.973	5.778	4.974	4.989	5.100
H_3BO_3	6.448	6.502	6.023	5.958	5.855	5.391

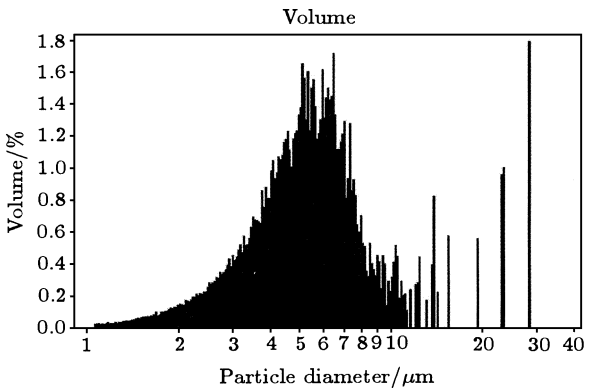


Fig.4. Particle size distribution of $Ba_{0.85}MgAl_{10}O_{16.94}:Eu^{2+}_{0.09}$ (no flux, T=1550°C).

The main parameters of particle size distribution with different fluxes are shown in Table 2 and the particle size distribution diagram (without flux, T=1550°C) is shown in Fig.4. The mean particle size of these phosphors is in the range from 4.428 to 6.428μm and the median particle size changes in the range from 4.646 to 6.502μm. Phosphors with this particle size are suitable for fluorescent lamps, cathode-ray tubes and x-ray intensifying screens.[16]

From Table 2 and Fig.5, it can be seen that when fluorides are selected as fluxes, the particle size is a little larger than that with chlorides as fluxes. With chlorides as fluxes at 1550°C firing temperature, the mean diameters of the samples are less than 5.0μm, which are smaller than that of the sample without

any flux (5.250μm). In contrast, with the fluorides as fluxes, the mean diameters are greater than 6.0μm (except the case with BaF_2 as flux: 5.789μm), which are larger than the ones without any flux and with chlorides as fluxes. The samples with H_3BO_3 as flux also have a larger particle size with the mean diameter of 6.448μm at 1550°C firing temperature. Generally, the higher the firing temperature is, the larger the particle size will be. However, it is difficult to understand that the samples with chlorides as fluxes have a relatively smaller particle size at higher firing temperature (1550°C) but have a larger particle size at the lower firing temperature (1400°C), as shown in Fig.5.

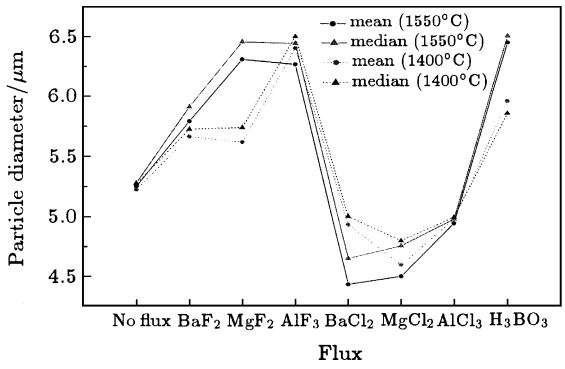


Fig.5. Particle size of $Ba_{0.85}MgAl_{10}O_{16.94}:Eu^{2+}_{0.09}$ with different fluxes.

3.3. Luminescence characteristics of the phosphors

3.3.1. Emission characteristics under 254nm excitation

Figure 6 shows the excitation spectra (λ_{em}= 450nm) of $Ba_{0.85}MgAl_{10}O_{16.94}:Eu^{2+}_{0.09}$ prepared with different fluxes. The excitation spectrum of the blue fluorescence shows two wide bands with peaks near 277nm and 310nm, respectively, owing to the crystal field splitting of the Eu^{2+} d-orbital.[4,17] The properties of Eu^{2+} and Eu^{3+} have been investigated in some material systems in literature.[18–22] It can be seen from Fig.6 that for the samples at 1550°C firing temperature there are strongest peaks near 277nm. However, the strongest peaks appear near 310nm when the samples are fired at 1400°C.

Figures 7 and 8 show the emission spectra (λ_{ex}=254nm) of $Ba_{0.85}MgAl_{10}O_{16.94}:Eu^{2+}_{0.09}$ with different fluxes at different firing temperature (1400°C and 1550°C). These spectra contain broad band emission with peaks near 450nm and halfwidths about 50nm, which corresponds to $4f^65d$–$4f^7$ transition of the Eu^{2+} ion. This broad band emission was thought to be caused by a variety of factors acting either separately or jointly: namely, multiple luminescent sites, high inhomogeneity, strong electron–phonon coupling, reabsorption of emission of one (or more) sites, etc.[1,8]

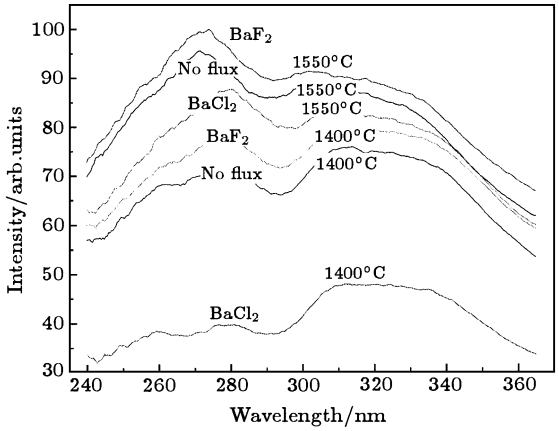


Fig.6. Excitation spectra of $Ba_{0.85}MgAl_{10}O_{16.94}:Eu^{2+}_{0.09}$ with different fluxes.

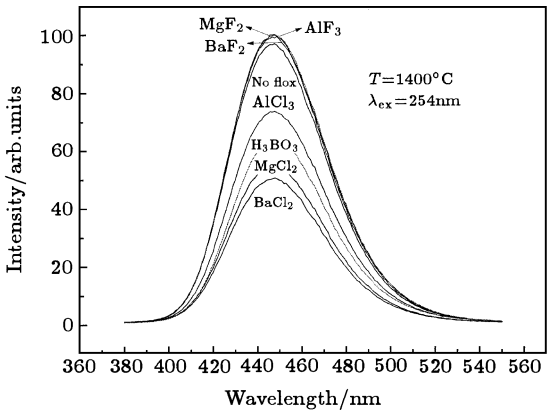


Fig.7. Emission spectra of $Ba_{0.85}MgAl_{10}O_{16.94}:Eu^{2+}_{0.09}$ with different fluxes.

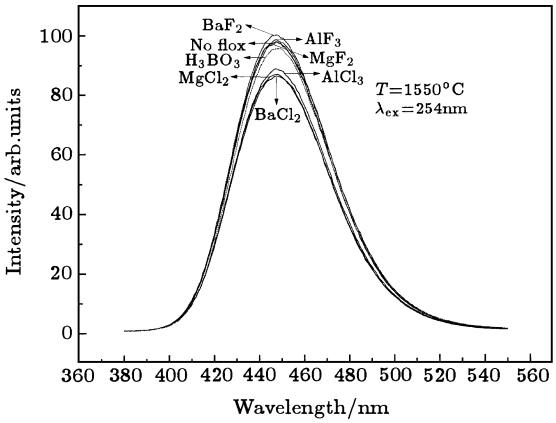


Fig.8. Emission spectra of $Ba_{0.85}MgAl_{10}O_{16.94}:Eu^{2+}_{0.09}$ with different fluxes.

From Figs.7 and 8, the emission spectra can be divided into two groups according to their relative emission intensities. One is the fluoride group and the other is the chloride group. The former group has higher relative emission intensities and the latter group has lower relative emission intensities. The relative emission intensities of samples without flux or with H_3BO_3 as flux fall between those of the two groups, which is obvious in Fig.9 and Table 3. Therefore, the conclusion can be drawn that the fluorides have better flux effects than chlorides and H_3BO_3.

Table 3. Relative emission intensities and CIE coordinates of $Ba_{0.85}MgAl_{10}O_{16.94}:Eu^{2+}_{0.09}$ with different fluxes.

Flux	Fired at 1550°C (254nm excitation)			Fired at 1400°C (254nm excitation)		
	CIE coordinates		Relative	CIE coordinates		Relative
	x	y	intensities	x	y	intensities
No Flux	0.1466	0.0542	92.1	0.1470	0.0510	85.4
BaF_2	0.1478	0.0575	100.0	0.1468	0.0519	89.0
MgF_2	0.1467	0.0556	97.6	0.1467	0.0529	90.0
AlF_3	0.1472	0.0575	98.5	0.1464	0.0533	89.8
$BaCl_2$	0.1443	0.0604	86.2	0.1474	0.0517	45.5
$MgCl_2$	0.1464	0.0541	86.7	0.1473	0.0517	49.7
$AlCl_3$	0.1462	0.0547	88.6	0.1469	0.0538	66.3
H_3BO_3	0.1459	0.0565	95.4	0.1466	0.0565	57.9

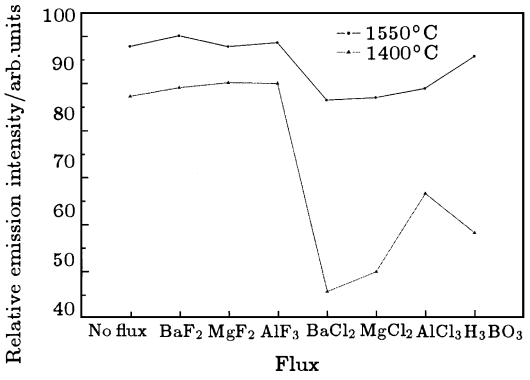


Fig.9. Relative emission intensities of $Ba_{0.85}MgAl_{10}O_{16.94}:Eu^{2+}_{0.09}$ with different fluxes.

Table 3 gives the relative emission intensities and corresponding CIE chromaticity coordinates of $Ba_{0.85}MgAl_{10}O_{16.94}:Eu^{2+}_{0.09}$ with different fluxes. The relative emission intensities are consistent with the results shown in Fig.9 when excited at 254nm. As far as the CIE chromaticity coordinates are concerned, it is generally agreed that the lower the y value is, the better performance the blue emitting phosphor has. Phosphors are practical with y values between 0.06 and 0.10.[23] Phosphors with high y values are usually thought to have poor thermal stability and some other defects. From Table 3, it can be seen that the phosphors have relatively stable x values (0.1443–0.1472) and preferable y values (0.0510–0.0605) regardless of flux type and firing temperature.

There has been no detailed report on the function of fluxes in the mechanism of $BaMgAl_{10}O_{17}:Eu^{2+}$ particle growth.[24] However, it is generally agreed that fluxes are usually compounds of alkali or alkaline earth metals having low melting points and when the fluxes melt, the surface tension of liquid helps particles to coagulate. The melt also makes it easier for particles to slide and rotate, provides more chances of particle–particle contacts, and promotes particle growth.[15] Flux accelerates the crystal growth, and sometimes flux can reduce the activation energy of the crystal growth in some phosphor preparation, such as in the firing process of zinc sulfide phosphors.

When fluorides are used as fluxes, the possible mechanism of $BaMgAl_{10}O_{17}:Eu^{2+}$ particle growth is proposed as follows. The following reaction will occur when the raw materials are being fired:

$$\begin{aligned} &BaCO_3 + MgO + (4/3)AlF_3 \rightarrow \\ &BaMgF_4 + (2/3)Al_2O_3 + CO_2, \\ &BaMgF_4 + (17/3)Al_2O_3 \rightarrow \\ &BaMgAl_{10}O_{17} + (4/3)AlF_3; \end{aligned} \tag{1}$$

$$\begin{aligned} &MgO + 2BaF_2 \rightarrow BaMgF_4 + BaO, \\ &BaMgF_4 + 5Al_2O_3 + 2BaO \rightarrow \\ &BaMgAl_{10}O_{17} + 2BaF_2; \end{aligned} \tag{2}$$

$$\begin{aligned} &BaCO_3 + 2MgF_2 \rightarrow BaMgF_4 + MgO + CO_2, \\ &BaMgF_4 + 5Al_2O_3 + 2MgO \rightarrow \\ &BaMgAl_{10}O_{17} + 2MgF_2. \end{aligned} \tag{3}$$

The Eu^{2+} ions are introduced from Eu_2O_3

when fired in a reducing atmosphere. As the above chemical equations show, the fluoride reacts with some components in raw material and begins to produce $BaMgF_4:Eu^{2+}$ at around 1000°C through solid-state reaction. The $BaMgF_4:Eu^{2+}$ melts at temperature over 1000°C. So the reaction will continue in $BaMgF_4:Eu^{2+}$ solutions and more and more $BaMgF_4:Eu^{2+}$ will be produced above 1000°C. $BaMgAl_{10}O_{17}:Eu^{2+}$ will begin to be created in $BaMgF_4:Eu^{2+}$ solutions at around 1200°C with AlF_3, BaF_2 or MgF_2 being recreated. Above 1200°C, the $BaMgF_4:Eu^{2+}$ will decrease with the increase of firing temperature and more and more $BaMgAl_{10}O_{17}:Eu^{2+}$ will be created with more AlF_3, BaF_2 or MgF_2 reformed. At around 1600°C, the $BaMgAl_{10}O_{17}:Eu^{2+}$ are created completely and will not increase with the increase of firing temperature. Our assumption is strongly supported by the experiment of Oshio's group.[24–26] In their experiment, the melting point of $BaMgF_4:Eu^{2+}$ had been proved at around 900–1000°C. They also studied the process that AlF_3 decomposed $BaMgAl_{10}O_{17}:Eu^{2+}$ phosphor into the mixture of $BaMgF_4:Eu^{2+}$ and Al_2O_3 and the process of recreation of $BaMgAl_{10}O_{17}:Eu^{2+}$ and AlF_3 with the increase of firing temperature by XRD and SEM. It was found that the XRD intensities of $BaMgAl_{10}O_{17}:Eu^{2+}$ and AlF_3 decreased with the increase of firing temperature and the intensity of $BaMgAl_{10}O_{17}:Eu^{2+}$ approached zero at 1000°C. However, the intensities of $BaMgF_4:Eu^{2+}$ and Al_2O_3 took place concurrently with a decrease in the intensities of AlF_3 and the decomposition of $BaMgAl_{10}O_{17}:Eu^{2+}$. Then the intensity of $BaMgF_4:Eu^{2+}$ increased continuously with the increase of firing temperature and peaked at 1200°C. Subsequently, the x-ray diffraction peak of $BaMgAl_{10}O_{17}:Eu^{2+}$ reappeared and the intensity had a notable increase relative to decreasing the $BaMgF_4:Eu^{2+}$ and Al_2O_3 over 1200°C and this process ended at 1600°C.

As for the reformed AlF_3, BaF_2, MgF_2, part of the reformed AlF_3 was considered to sublimate for it is a material which has a sublimating point at 1273°C.[24] The rest of AlF_3 and reformed BaF_2 and MgF_2 will enter the host lattice and form the new luminescent centre $Eu^{2+}(F^-)$, from which there exists effective energy transfer to $Eu^{2+}(O^{2-})$, and it is helpful to improve the quenching concentration of Eu^{2+} in $BaMgAl_{10}O_{17}:Eu^{2+}$ phosphor.[2]

Concerning the function of chlorides as fluxes in the process of $BaMgAl_{10}O_{17}:Eu^{2+}$ particle growth, it remains unknown. But in view of the relative small particle size compared to the case of fluorides as fluxes, it may be disadvantageous for $BaMgAl_{10}O_{17}:Eu^{2+}$ particle growth to add chlorides as fluxes, which also can obtain evidence from the relatively low emission intensities with chlorides as fluxes.

3.3.2. Emission characteristics under 147nm excitation

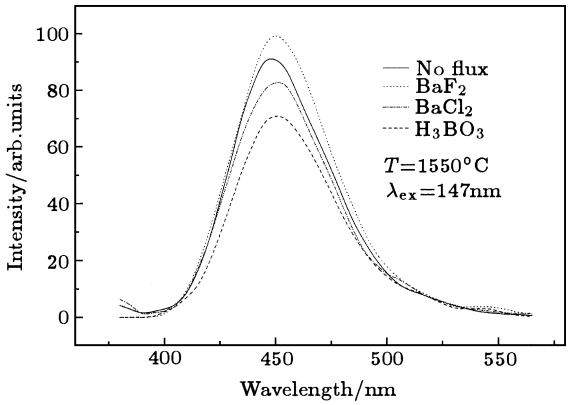


Fig.10. Emission spectra of $Ba_{0.85}MgAl_{10}O_{16.94}:Eu^{2+}_{0.09}$ with different fluxes.

As $BaMgAl_{10}O_{17}:Eu^{2+}$ phosphor is used as a blue-emitting phosphor for plasma display panels; VUV excitation is required for this display pattern. The emission characteristics of $Ba_{0.85}MgAl_{10}O_{16.94}:Eu^{2+}_{0.09}$ are studied under 147nm excitation. The emission spectrum is shown in Fig.10 and the relative emission intensities and CIE chromaticity coordinates are listed in Table 4. The emission spectrum also has a broad band emission with the peak at about 450nm which is similar to the one excited at 254nm. The spectra always resemble each other in shape regardless of flux type, but it differs in emission intensity (shown in Table 4). Similar to the case under 254nm excitation, the emission spectra can be divided into two groups according to their relative emission intensities. One is the fluoride group and the other is chloride group. The fluoride group has higher relative emission intensities and the chloride group has much lower relative emission intensities. The relative emission intensities of samples without any flux fall between those of the two groups, which is obvious from Fig.10 and Table 4. However, the sample with H_3BO_3 as flux has lowest emission intensity. Therefore, similarly, the conclusion can be drawn that the fluorides have better flux effects than chlorides and H_3BO_3 as flux has the poorest flux effect in the preparation of blue emitting phosphors for PDP. As for the CIE chromaticity coordinates under VUV excitation, the phos-

phors show relatively stable x values and preferable y values too, but the y values have a slight rise compared with the case under 254nm excitation.

Table 4. Relative emission intensities and CIE coordinates of $Ba_{0.85}MgAl_{10}O_{16.94}:Eu^{2+}_{0.09}$ with different fluxes.

Flux	Fired at 1550°C (147nm excitation)		
	CIE coordinates		Relative
	x	y	intensities
No Flux	0.1468	0.0586	91.1
BaF_2	0.1489	0.0647	100.0
MgF_2	0.1464	0.0631	98.4
AlF_3	0.1483	0.0684	84.8
$BaCl_2$	0.1484	0.0640	82.9
$MgCl_2$	0.1476	0.0642	81.6
$AlCl_3$	0.1461	0.0637	81.7
H_3BO_3	0.1448	0.0662	71.2

4. Conclusions

The $Ba_{0.85}MgAl_{10}O_{16.94}:Eu^{2+}_{0.09}$ phosphors with different fluxes were prepared by high temperature solid-state reaction method and their luminescence characteristics were studied under 254nm excitation and VUV (147nm) excitation. All the samples were found by XRD technique to have the single β-alumina structure and similar crystallinities regardless of the flux type. The samples with fluorides as fluxes have larger particle size than the samples with chlorides. When under 254nm and 147nm excitation, there is a similar emission spectrum in the shape regardless of flux type; both have a broad band emission with the peak at about 450nm. The fluxes can be divided into two groups according to the relative emission intensities and the fluoride group has better flux effects than the chloride group. In addition, the mechanism of $BaMgAl_{10}O_{17}:Eu^{2+}$ particle growth with fluorides as fluxes was proposed and discussed in detail.

References

[1] Ellens A, Zwaschka F, Kummer F, Meijerink A, Raukas M and Mishara K 2001 *J. Lumin.* **93** 147

[2] Liu Y L and Shi C S 2001 *Mater. Res. Bull.* **36** 109

[3] Yokota K, Zhang S, Kimura K and Sakamoto A 2001 *J. Lumin.* **92** 223

[4] Yu Z J, Zhuang W D, Zhao C L, Chang Y F, Huang X W, He H Q, Zeng D D and Han J X 2001 *J. Chin. Rare Earth Soc.* **19** 590

[5] Zhang J Y, Zhang Z T, Tang Z L, Zheng Z S and Lin Y H 2002 *Power Technol.* **126** 161

[6] Shionoya S, Yen W M, Hase T, Kamiya S, Nakazawa E, Narita K, Ohno K, Weber M and Yamamoto H 2000 *Phosphor Handbook* (New York: CRC Press) pp416–17

[7] Kim Y I, Kim K B, Jung M J and Hong J S 2002 *J. Lumin.* **99** 91

[8] Mishra K C, Raukas M, Ellens A and Johnson K H 2002 *J. Lumin.* **96** 95

[9] Iyi N, Göbbels M and Kimura S 1998 *J. Solid State Chem.* **136** 258

[10] Shionoya S, Yen W M, Hase T, Kamiya S, Nakazawa E, Narita K, Ohno K, Weber M and Yamamoto H 2000 *Phosphor Handbook* (New York: CRC Press) p833

[11] Smets B M J and Verlijsdonk J G 1986 *Mater. Res. Bull.* **21** 1305

[12] Verstegen J M P J and Stevels A L N 1974 *J. Lumin.* **19** 406

[13] Ravichandran D, Johnson S T, Erdei S, Roy R and White W B 1999 *Displays* **19** 197

[14] Stevels A L N and Schrama-de Pauw A D M 1976 *J. Electrochem. Soc.* **123** 691

[15] Shionoya S, Yen W M, Hase T, Kamiya S, Nakazawa E, Narita K, Ohno K, Weber M and Yamamoto H 2000 *Phosphor Handbook* (New York: CRC Press) p323

[16] Shionoya S, Yen W M, Hase T, Kamiya S, Nakazawa E, Narita K, Ohno K, Weber M and Yamamoto H 2000 *Phosphor Handbook* (New York: CRC Press) p328

[17] Ronda C R and Smets B M J 1989 *J. Electrochem. Soc.* **136** 570

[18] He Z Y, Wang Y S, Sun L and Xu X R 2000 *Acta Phys. Sin.* **49** 1377 (in Chinese)

[19] Jia D D, Wu B Q and Zhu J 2000 *Acta Phys. Sin.* **9** 69 (in Chinese)

[20] Jia D D, Wu B Q and Zhu J 1999 *Chin. Phys.* **8** 813

[21] Yang X J, Si C S and Xu X L 2002 *Acta Phys. Sin.* **51** 2871 (in Chinese)

[22] Song F, Tan H and Zhang G Y 2002 *Acta Phys. Sin.* **51** 2375 (in Chinese)

[23] Wu L Q, Zhang J B, Zhang J F and Qiu G X 1998 *Chin. J. Lumin.* **19** 251

[24] Oshio S, Matsuoka T, Tanaka S and Kobayashi H 1998 *J. Electrochem. Soc.* 145 3898

[25] Oshio S, Matsuoka T, Tanaka S and Kobayashi H 1998 *J. Electrochem. Soc.* **145** 3903

[26] Oshio S, Kitamura K, Nishiura T, Shigeta T, Horii S and Matsuoka T 1997 *National Technical Report* (Matsushita Electric Industry Company) **43** 69